Distribution coefficients of 60 elements on TODGA resin: Application to Ca, Lu, Hf, U and Th isotope geochemistry

Ali Pourmand[*], Nicolas Dauphas

Origins Laboratory, Department of the Geophysical Sciences and Enrico Fermi Institute, The University of Chicago, 5734 South Ellis Avenue, Chicago, IL 60637, USA

ARTICLE INFO

ABSTRACT

Batch equilibration experiments are conducted to measure the distribution coefficients (K_d) of a large number of elements in nitric, nitric plus hydrofluoric, and hydrochloric acids on Eichrom TODGA extraction chromatography resin. The K_ds are used to devise a multi-element extraction scheme for high-precision elemental and isotopic analyses of Ca, Hf, Lu, Th and U in geological materials, using high-purity lithium metaborate ($LiBO_2$) flux fusion that allows rapid digestion of even the most refractory materials. The fusion melt, dissolved in nitric acid, is directly loaded to a TODGA cartridge on a vacuum chamber for elemental separation. An Ln-Spec cartridge is used in tandem with TODGA for Lu purification. The entire procedure, from flux digestion to preparation for isotopic analysis, can be completed in a day. The accuracy of the proposed technique is tested by measuring the concentrations of Ca (standard bracketing), Hf, Lu, Th and U (isotope dilution), and the isotopic composition of Hf in geostandards (USNM3529, BCR-2, BHVO-1, AGV-1 and AGV-2). All measurements are in excellent agreement with recommended literature values, demonstrating the effectiveness of the proposed analytical procedure and the versatility of TODGA resin.

© 2010 Elsevier B.V. All rights reserved.

1. Introduction

The advent of commercial high-resolution multi-collector inductively coupled plasma mass spectrometers (HR-MC-ICP-MS) has lead to significant advances in high-precision elemental and isotopic analyses of terrestrial and extraterrestrial materials [1–5]. It is well-documented that the presence of matrix elements and molecular interferences can create systematic and stochastic effects on instrumental mass bias and ion detection in ICP-MS, which may cause significant analytical artifacts [6–9]. Sample purification (*i.e.*, isolating the analytes of interest from the matrix prior to analysis), is therefore an essential prerequisite to conducting precise and accurate elemental and isotopic measurements with (MC)-ICP-MS.

Numerous procedures have been developed over the last few decades that utilize the distribution coefficient of elements on ion exchange resins to achieve quantitative elemental separation [10–16]. These procedures often involve slow, gravity-driven elution of elements in different acid mixtures. An alternative to this approach is to use a combination of solvent extraction and column chromatography. Since the early 1990s, Eichrom Technologies Inc. (hereafter Eichrom) has developed a series of extraction chromatography resins that are specifically designed to separate trans-uranium elements from natural and nuclear waste material [17,18]. The applications of these and other solvent extraction chromatography resins, however, are not limited to the nuclear industry or radiochemistry, and there has been a growing interest within the geochemistry community in recent years to use these resins for analytical separation of elements in natural materials [19–25].

A late addition to the inventory of commercially available extraction chromatography resins from Eichrom is a synthesized tridentate ligand known as *N,N,N′N′* tetraoctyl-1,5-diglycolamide (hereafter TODGA). TODGA extractant has been traditionally used in high-level radioactive waste procurement of trivalent lanthanides, actinides and other fission products [26–29]. TODGA has also been successfully utilized in conjunction with other ion exchange or solvent extraction resins to purify high-field strength elements (HFSE) and rare earth elements (REE) in rocks [30–33]. In spite of the recent interest in this versatile resin, the full potential of TODGA and its prospective applications to the broad field of analytical geochemistry remain largely unexplored.

In the first part of this study, distribution coefficients for a large group of elements on TODGA resin are presented in various concentrations of HCl, HNO_3 and HF. In the second part, elution curves and extraction chromatography separation schemes are devised based on the distribution coefficients of a select group of elements

on TODGA and Ln-Spec resins. Finally, a rapid and robust analytical procedure is proposed with low-blank flux fusion and vacuum cartridge chromatography for high-precision isotopic and elemental analyses of Ca, Lu, Hf, U, and Th in natural samples. The entire analytical procedure, from digestion to preparation for analysis on MC-ICP-MS can be completed in a day.

2. Experimental

2.1. Analytical material, standards and reagents

Analytical grade ACS Plus HCl and HNO_3 (Fisher Scientific) were double-distilled in sub-boiling silica glass and PTFE Teflon distillation units, and were titrated before dilution. High-purity HF OPTIMA (Fisher Scientific) was used without further distillation. All Teflon labware was pre-cleaned in two stages: first with sub-boiling 50% HNO_3, followed by boiling in a 3:1 mixture of $HCl:HNO_3$. Single and multi-element ICP-MS standard solutions (Spex CertiPrep) were obtained at concentrations of 10 ± 0.05 and $1000 \pm 5 \, \mu g \, mL^{-1}$. Pre-packed, 2-mL cartridges containing TODGA resin (particle size 50–100 μm) were purchased from Eichrom. Disposable polypropylene tubes (Corning) and polypropylene columns (Bio-Rad) were used to perform equilibration experiments, filtration and final dilutions for elemental concentration analyses on the ICP-MS. Batch experiments were conducted inside a clean laboratory at an ambient temperature of 22–24 °C. Milli-Q water (Millipore, resistivity > 18 $M\Omega \, cm^{-1}$) was used for all acid dilutions.

2.2. Distribution coefficient of elements on TODGA resin

The distribution coefficient (K_d) quantifies the partition of an element between the acid solution (mobile phase) and the extractant (stationary phase):

$$\text{distribution coefficient} \, (K_d) = \frac{C_{solid} \text{ per gram TODGA}}{C_{solution} \text{ per mL solution}} \quad (1)$$

C_{solid} is the concentration of elements attached to the resin, in micrograms per gram of dry TODGA resin, and $C_{solution}$ is the concentration of ions, in micrograms per mL of solution, which remains in solution after equilibration is established between the acid and the resin. Single and multi-element standards are commercially available in combinations of dilute HF, H_2O_2, HCl, HNO_3 and $C_4H_6O_6$ (tartaric acid) solutions. The presence of these acids in the mobile phase during the resin-solution equilibration can potentially modify the partition behavior of elements in TODGA extractant. Even trace amounts of HF, for instance, are known to dramatically reduce the affinity of Hf for TODGA extractant [32]. In order to avoid this problem during equilibration experiments, aliquots of commercially manufactured standard solutions were transferred to a pre-cleaned, 125 mL Savillex PFA beaker and the mixture was evaporated to dryness inside a class-100 laminar flow hood. After complete evaporation, the solid residue was dissolved in concentrated HNO_3 or HCl and the process was repeated three times to ensure complete removal of other acids.

In preparation of each batch for equilibration experiments, about 300 mg of dry TODGA resin was transferred from 2 mL cartridges to 15 mL centrifuge tubes. An aliquot of the stock multi-element standard solution was diluted with MQ-water in a pre-cleaned Savillex beaker and the acid concentration was adjusted with additional HCl, HNO_3 or HF. The mixture in 5–10 mL was directly added to the TODGA resin. Batch experiments were conducted for 60 elements in 0.1, 1, 3, 6, 9 and 12 mol L^{-1} HNO_3, 58 elements in 0.1, 1, 3, 6, 9 and 10 mol L^{-1} HCl, and 12 elements in 0.1, 1, 3, 6, 9 and 12 mol L^{-1} HNO_3 + 0.2 mol L^{-1} HF. The HNO_3 + HF experiments were specifically conducted to develop a chromatography scheme to separate Ca, U, Th, Lu and Hf from rock matrices

(Section 3). A blank solution was prepared with each batch of equilibration experiment, and analyzed together with the samples. The resin and the acid-standard solution were stirred by placing the vials on a Thermoline Vortex shaker ($\sim$1000 rpm) for 5–10 min every 2 h. After 8 h of equilibration, the mixture was filtered using pre-cleaned, 2-mL Bio-Rad columns fitted with frits, to separate the resin from the mobile phase. The acid solutions were collected in centrifuge tubes and were diluted by factors of 10–100 in 0.4 mol L^{-1} HNO_3 or HCl prior to analysis.

Measurements were performed on a ThermoFinnigan Neptune MC-ICP-MS at the Origins Lab of the University of Chicago. The solutions were introduced into the Neptune using a 100 $\mu L \, min^{-1}$ PFA Teflon self-aspirating nebulizer. A combined ESI quartz cyclonic and Scott-type Stable Introduction System (SIS) was used for all distribution coefficient measurements. Representative isotopes were selected with preference given to higher relative abundances and absence of isobaric interferences. Elemental concentrations were determined by bracketing each batch of samples with a multi-element standard solution. The procedural blank and acid contributions (generally below 1%) were subtracted from each analysis. An extended form of Eq. (1) was used to determine the distribution coefficients for each element:

$$K_d = \frac{(C_B - C_A)/w}{C_A/V} \quad (2)$$

C_B and C_A are the elemental concentrations in micrograms per mL of solution before and after equilibration, respectively, w is the weight of dry TODGA resin in grams and V is the volume of acid solution in milliliters. Equilibration experiments were replicated using freshly prepared multi-element standard solutions, and the final distribution coefficients were calculated based on the geometric averages of replicate analyses. The difference of logarithmic K_ds between two equilibration experiments was better than 3% for most elements.

Figs. 1–3 show the partition coefficients (logarithmic scale) on TODGA as a function of HCl, HNO_3 and HNO_3 + 0.2 mol L^{-1} HF concentrations. A high K_d value at a specific acid concentration means the ion is preferentially retained on the resin, while a low K_d indicates the release of the ions to the mobile phase (acid solution). Although partial separation can be potentially achieved at K_d > 1, large differentials in distribution coefficients are required for quantitative separation of analytes from matrix elements in natural samples.

Previously, Horwitz et al. [33] studied some of the properties of TODGA and TEHDGA extraction chromatography resins in slurry-packed gravity columns to explore the potential application of these resins. In addition to presenting the distribution coefficients of elements studied by these authors, we report K_ds for 30 new elements, including most transition and poor metals. For instance, the chromatographic behavior of Hf on TODGA, which was not studied by Horwitz et al. [33], plays a pivotal role in developing a separation scheme for Hf isotope analysis. Furthermore, the K_d of 12 elements in HNO_3 + 0.2 mol L^{-1} HF are also presented here and the HNO_3 and HCl concentrations for all experiments are extended to 12 and 10 mol L^{-1}, respectively. After converting the "resin capacity factor" from Horwitz et al. [33] to distribution coefficients (Eq. (2)), the partitioning behavior of most commonly studied elements on TODGA resin are comparable between the two studies. There are, however, some exceptions; Horwitz et al. [33] report that Fe(III) and Ti(IV) remain in the mobile phase in all concentrations of HNO_3. This is not observed in our study, as the Log K_d for Fe(III) and Ti(IV) consistently increases to $\sim$2 as a function of increasing HNO_3 concentration (Fig. 1). A possible explanation for the some of the discrepancies may be that Horwitz et al. [33] appear to have utilized metal ions directly from the original standard solutions in HCl and HNO_3 to conduct batch equilibration experiments. In contrast, a stock solution prepared by converting all standards to HCl and
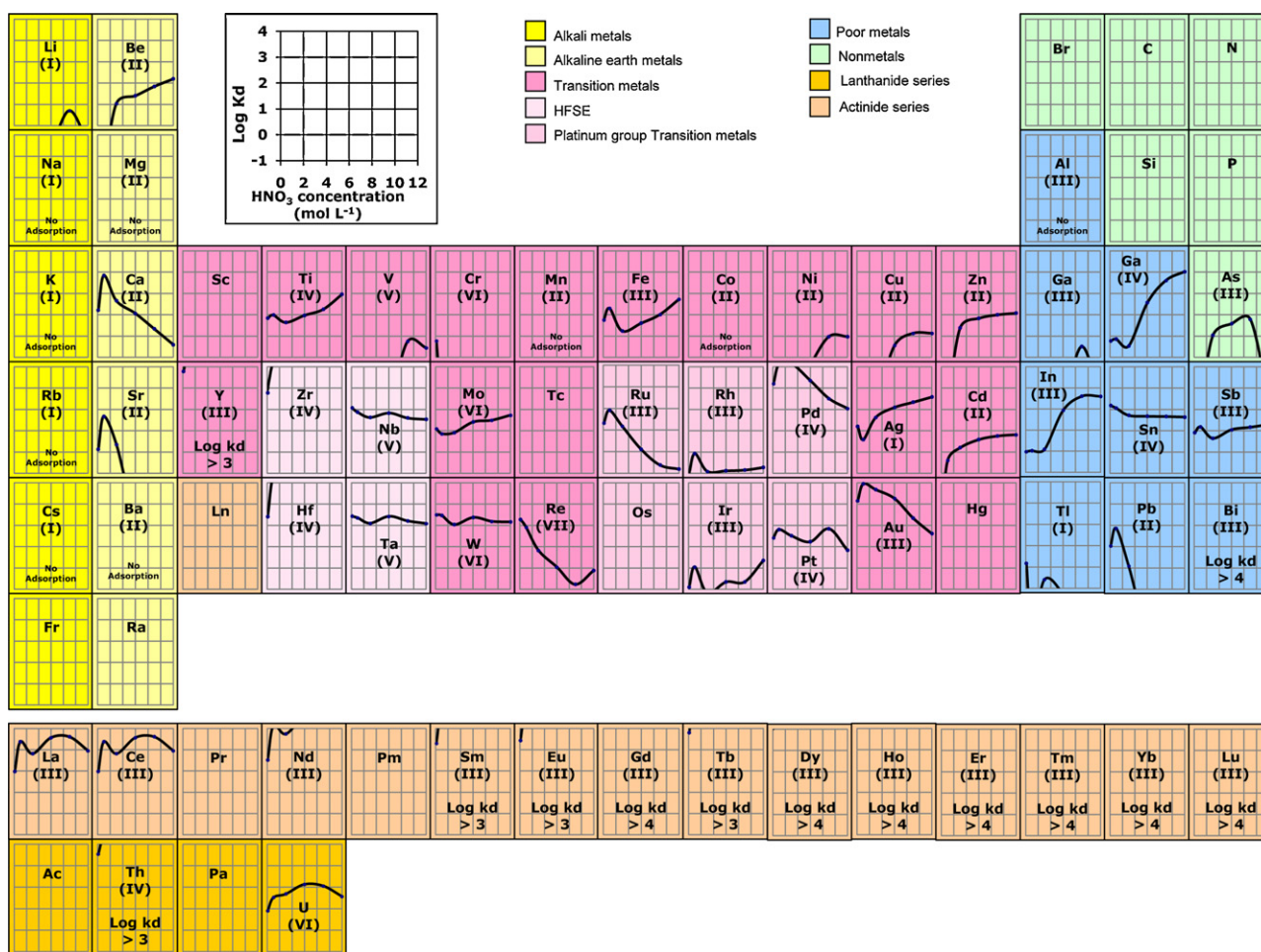
Fig. 1. Distribution coefficients (K_d) of 60 elements on TODGA resin in logarithmic scale as a function of HNO_3 molarity (measured at 0.1, 1, 3, 6, 9 and 12 mol L^{-1}). The six data points used to establish each curve are the geometric averages of two replicate analyses.

HNO_3 was used for experiments in this study. As evidenced by the behavior of Hf in the presence of trace amounts of HF (Fig. 3) [32], it is imperative for some elements to conduct equilibration experiments in the absence of any other compound that may impact the distribution coefficients on TODGA.

3. TODGA application: a novel flux fusion and vacuum extraction protocol

The elemental and isotopic composition of alkaline earth elements, high-field strength elements (HFSE), lanthanides and actinides in terrestrial and extraterrestrial material continue to advance our understanding of the processes involved in the evolution of the earth and other bodies in the solar system [23,34–37]. A variety of sample processing methods have been successfully developed using high-pressure Parr bomb HF dissolution, alkali flux fusions in conjunction with Eichrom extraction chromatography (TEVA, TRU-Spec, Ln-Spec and TODGA) and ion exchange resins [19,25,30,37–42]. Most of the existing protocols, however, require multiple evaporations and slow slurry-packed gravity chromatography separation steps.

In the following sections, the TODGA distribution coefficients are utilized to develop a simple method of sample digestion and extraction chromatography for concomitant separation of U, Th, Ca, Hf, Lu and Yb for MC-ICP-MS analyses. Results from Parr bomb dissolution and lithium metaborate flux fusion in platinum and high-purity graphite crucibles are compared. Aliquots of

Allende standard reference powder from the Smithsonian Institute (USNM3529, Split 8, Position 5, homogenized from 4 kg, hereafter USNM3529) and a suite of geostandards were analyzed and the results were compared with recommended literature values to evaluate the suitability of our proposed protocol for high-precision analyses of extraterrestrial and geological material.

The proposed analytical procedure has several advantages: (a) complete dissolution of refractory phases (such as zircons) is ensured by fusing the sample with a purified, low-blank borate flux at 1070 °C in less than 12 min, (b) molten sample readily dissolves in acid and is directly loaded onto extraction chromatography columns without further processing, (c) high efficiency vacuum cartridge extraction chromatography allows fast elemental separations at unprecedented high flow rates with complete removal of all matrix elements and isobaric interferences, (d) a single TODGA cartridge is used for separation of U, Th, Ca and Hf with no need for further purification, (e) Lu is isolated from residual low and middle mass lanthanides with a single Ln-Spec cartridge used in tandem with TODGA and finally, (f) the entire procedure, from sample digestion to MC-ICP-MS analysis, can be completed in a day.

3.1. Spike calibration

The elemental concentrations of Lu, Hf, U and Th in standard reference materials were measured using isotope dilution mass spectrometry [43,44] using a calibrated multi-spike solution that
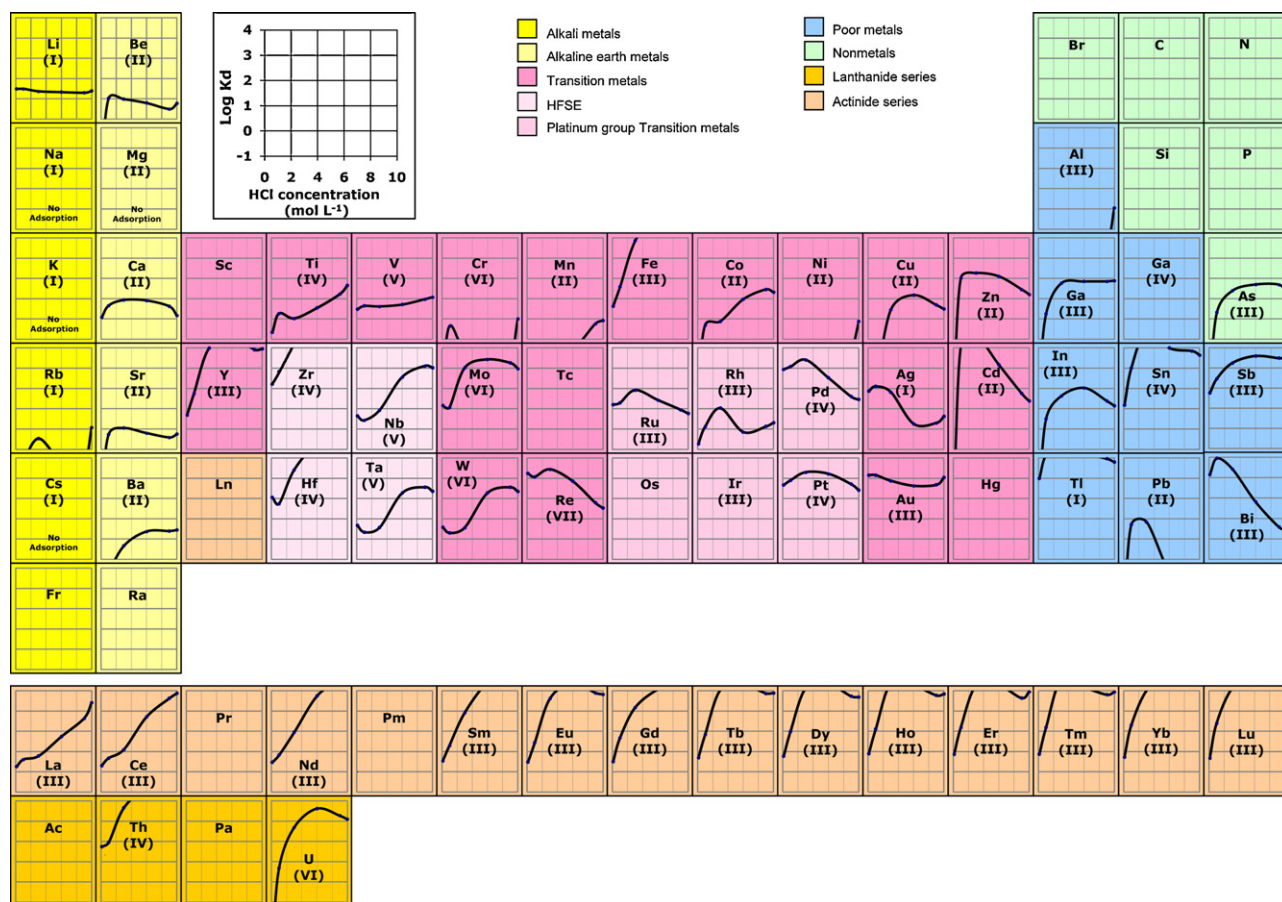
Fig. 2. Distribution coefficients (K_d) of 58 elements on TODGA resin in logarithmic scale as a function of HCl molarity (measured at 0.1, 1, 3, 6, 9 and 10 mol L^{-1}). The six data points used to establish each curve are the geometric average of two replicate analyses.

contained enriched ^{176}Lu, ^{180}Hf, ^{229}Th and ^{236}U isotopes. Enriched ^{176}Lu and ^{180}Hf isotopes were obtained from Oakridge National Lab in the form of LuO$_2$ and HfO$_2$ powders. LuO$_2$ was readily dissolved in 3 mol L^{-1} HNO$_3$ while complete dissolution of HfO$_2$ required a more rigorous treatment with Parr bomb and HF at 140 °C for 8 h. The ^{229}Th and ^{236}U spikes were provided courtesy of Franco Marcantonio at Texas A&M University. A mixed multi-spike solution of ^{176}Lu–^{180}Hf–^{229}Th–^{236}U was prepared and concentration of the spike components were calibrated by reverse isotope dilution against gravimetrically prepared Lu–Hf–U–Th standard solutions from certified mono-elemental standards (1000 ± 5 μg mL^{-1}, Spex CertiPrep). Table 1 shows the composition and abundances of the isotopes in the final multi-spike solution.
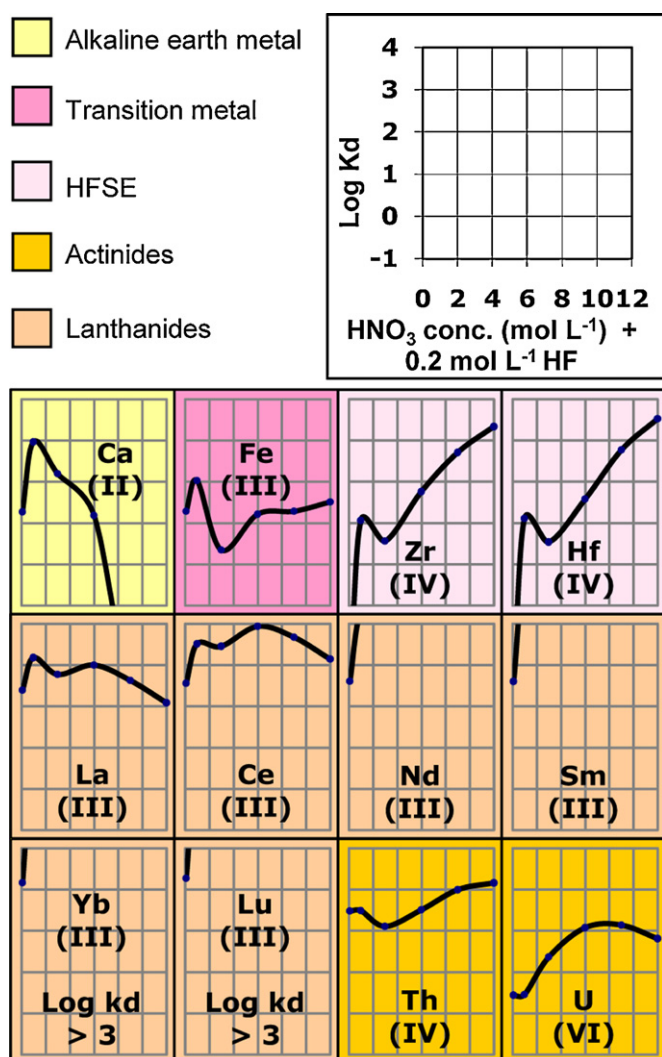
3.2. Sample digestion

3.2.1. High-purity borate flux fusion

Fusion with borate fluxes at temperatures exceeding 1000 °C is a highly effective way to digest rocks and sediment samples, and has clear advantages over conventional hotplate or Parr bomb acid dissolution methods [19,32,39,45]. High-temperature flux melting can be carried out within minutes and complete destruction of refractory phases is achieved. In comparison, both hotplate and high-pressure Parr bomb dissolutions require hours to days of treating the sample with hazardous acids such as HF, especially when large amounts of silicate minerals or refractory phases such as zircon and garnet are present. In fact, a recent study found that hotplate dissolution can produce inconsistent results due to incom-

plete sample dissolution and sample-spike equilibration [46]. In addition, dissolution in the presence of HF may lead to the formation of insoluble fluoride complexes [38] that require several dry-down and fuming steps, thereby increasing the risk of sample loss and elevated blanks due to contamination. Despite the obvious advantages of flux fusion, a major pitfall in utilizing this technique is the presence of high blanks, which is addressed in the following section.

3.2.2. Blank contribution from borate flux

The lithium metaborate flux fusion method of digestion can be inadequate for geological materials that require low levels of procedural blank. In order to take advantage of flux fusion in developing our analytical procedure to analyze Ca, U, Th, Hf and Lu in meteorites, the main sources of procedural blank were identified, and are reported in Table 2. Calcium blanks did not pose a problem, as the amount of Ca in about 100 mg of digested chondrites (average Ca concentration of 12.7 mg g^{-1} [47]) is nearly three orders of magnitude higher than the procedural blank of 1.6 μg (see Section 3.4). Measured Lu blanks were consistently below detection. It is evident from Table 2 that the main contributor to U, Th and Hf blank is the borate flux. Out of three "high-purity" grade borate fluxes that were analyzed, Puratronic Alfa Aesar (99.997%, Cat# 10739) flux had the lowest blanks but was still insufficient for low concentration measurements. A simple purification method was therefore developed to lower the blank levels in high-purity commercial borate flux.

Table 1
Isotopic composition of Hf, Lu, Th and U spikes in the multi-spike solution.

Isotope	Spike abundance (%)	Natural abundance (%)
Hafnium		
[174]Hf	0.00976	0.1620
[176]Hf	0.06202	5.2604
[177]Hf	0.25779	18.5953
[178]Hf	0.34701	27.2811
[179]Hf	0.18883	13.6210
[180]Hf	99.13459	35.0802
Lutetium		
[175]Lu	25.19709	97.4160
[176]Lu	74.80291	2.5840
Thorium		
[232]Th	1.66057	100.00
[229]Th	98.33943	0.00
Uranium		
[234]U	0.00090	0.0055
[235]U	0.01505	0.7200
[236]U	99.93011	0.0000
[238]U	0.05395	99.2745

Fig. 3. Distribution coefficients (K_d) of 12 elements on TODGA resin in logarithmic scale as a function of $0.2\,mol\,L^{-1}$ HF + HNO$_3$ molarity (measured at 0.1, 1, 3, 6, 9 and $12\,mol\,L^{-1}$ HNO$_3$). These curves were established to develop a matrix-analyte separation scheme for Ca, U, Th, Hf and Lu. High-field strength elements such as Hf are highly sensitive to the presence of trace amounts of HF on TODGA.

3.2.3. Purification of LiBO$_2$

The high affinities of Eichrom U/TEVA [18] and TODGA (Fig. 1) resins for U, Th and Hf in $3\,mol\,L^{-1}$ HNO$_3$ make it possible to effectively eliminate these elements from commercially manufactured borate flux. Approximately 60 g of Puratronic LiBO$_2$ (Alfa Aesar, 99.997% metal basis) was dissolved in 2 L of $3\,mol\,L^{-1}$ HNO$_3$ in a pre-cleaned, 2-L PFA Teflon bottle at room temperature (25 °C). A 2-mL U/TEVA (top) and two 2-mL TODGA cartridges (bottom) were stacked in tandem on an Eichrom vacuum chamber and 20 mL syringes were used as loading reservoirs. The cartridge assemblage was preconditioned with 60 mL of 65 °C $3\,mol\,L^{-1}$ HNO$_3$ + $0.3\,mol\,L^{-1}$ HF to remove resin impurities, followed by 20 mL of MQ-water and 20 mL of $3\,mol\,L^{-1}$ HNO$_3$ to convert to load acid condition. The dissolved flux was subsequently loaded to the cartridges and the purified solution was collected in pre-cleaned, 125-mL PFA Teflon bottles at a rate of 3–4 mL min^{-1}. Five U/TEVA-TODGA cartridge assemblies were used for the purification of ∼2 L of dissolved flux and the load volume per each array of cartridges was kept below 400 mL to avoid Hf, U and Th leakage from the resins.

The purified flux was recovered in two stages. The solution was first evaporated to a crust in increments of 200 mL inside pre-cleaned, 250 mL PFA Savillex® vessels capped with threaded closures with port holes to minimize contamination. To ensure complete dryness, the LiBO$_2$ crust was then transferred to a capped 100 mL platinum evaporation dish and heated in a Thermoline furnace for 45 min at 720 °C. The fully dried flux was transferred to a 250 mL PTFE Savillex vial and used for high-purity flux fusion. Sixty grams of the original LiBO$_2$ powder yielded approximately 50 g of purified flux.

3.2.4. Borate flux melting of reference material

Several experiments were conducted to determine the optimum flux:sample proportion to achieve complete digestion without excessive use of the flux. Although flux:sample ratios of 2:1 to 4:1 have previously been used [19,32,39,45], our fusion experiments with geostandards and meteorite powders showed that a minimum ratio of 6:1 is required to ensure complete sample digestion and subsequent dissolution of the flux in acid. Indeed, the complication reported elsewhere as "silica instability" [19] was only experienced when a small flux:sample ratio was used. Purified LiBO$_2$ flux was directly weighted into an ultra-pure 8 mL graphite crucible (Spex CertiPrep) and a small crater was created at the center of the powder to accommodate the sample. Approximately 150 mg of high-purity LiBr was added to the flux as a non-wetting agent, followed by the powdered standard reference material. Elemental blanks from LiBr were negligible (Table 2). The non-wetting agent eliminated the need for "pre-ignition" of the crucibles rec-

Table 2
Potential contributors to procedural blank. NA = not analyzed; <Det. = below detection.

Blank analyses	Hf (pg)	Lu (pg)	U (pg)	Th (pg)
LiBr (150 mg)	5	<Det.	6	8
$15\,mol\,L^{-1}$ HNO$_3$ (10 mL)	<Det.	<Det.	<Det.	<Det.
$10\,mol\,L^{-1}$ HCl (10 mL)	<Det.	<Det.	<Det.	<Det.
2 mL TODGA resin ($n = 3$)	31	<Det.	29	27
Savillex vials	<Det.	<Det.	<Det.	<Det.
Alfa Aesar LiBO$_2$, 99.997% purity (1 g)	138	<Det.	137	41
Alfa Aesar LiBO$_2$, 99.9% purity (1 g)	588	NA	1994	204687
Sigma–Aldrich LiBO$_2$, 99.95% purity (1 g)	28	NA	923	113
Pt crucible ($n = 6$)	93	NA	67	3
Glassy carbon crucible ($n = 2$)	42	NA	22	9
High-purity graphite crucible ($n = 2$)	21	<Det.	8	<Det.
Purified AE LiBO$_2$, 99.997% (1 g)	<Det.	<Det.	<Det.	<Det.

ommended by others [32,45], and facilitated transfer of the melt without loss to the crucible. This is a highly effective method for quantitative recovery of elements, which is particularly important for accurate concentration measurements with standard bracketing technique. The crucible was capped with a second graphite crucible to minimize contamination from the furnace, which can be quite significant, and fusion was performed at 1070 °C for 12 min. The melt was directly poured into 15 mL of 3 mol^{-1} L HNO$_3$ in a 30 mL PFA Savillex vial. The total volume was increased to 25 mL of 3 mol^{-1} L HNO$_3$. Complete dissolution was usually achieved within minutes of shaking the vial on a Thermoline Vortex at 1000 rpm, followed by ultra-sonication. Graphite fragments, examined under the microscope, were the only remaining residues. Approximately 100–200 mg of the ^{176}Lu–^{180}Hf–^{229}Th–^{236}U multi-spike solution was added and the sealed vial was heated at 90 °C for 4 h to achieve sample-spike equilibration prior to extraction chromatography.

3.2.5. Comparison with HF Parr bomb dissolution

An alternative method to flux fusion for digesting meteorites and terrestrial material is high-pressure Parr bomb dissolution using a mixture of HF and HNO$_3$ [46,48,49]. In order to compare the results from flux fusion with high-pressure acid dissolution, aliquots of reference materials were also digested with high-pressure Parr bombs. Approximately 10–100 mg of the standard powder was weighed into a clean 6 mL PFA Savillex vial. The calibrated spike mixture was added along with 4 g of HF and HNO$_3$ at a 3:1 ratio. The vial was heated inside a 45 mL PTFE Parr bomb at 160–170 °C for 5 days. The mixture was evaporated overnight at 90 °C and approximately 100 μL of HCLO$_4$ was added and fumed in several steps to convert insoluble fluorides to soluble compounds. The residue was finally dissolved in 4 g of concentrated HNO$_3$ and heated in the bomb for 5 days. In some cases, visible residues were still present and 2–5 days of additional heating were required to achieve complete dissolution. The HNO$_3$ partially evaporated during sample digestion so more concentrated nitric acid was added to the vial after sample dissolution and the final solution was adjusted to 25 mL of 3 mol L^{-1} HNO$_3$ + 0.2 mol L^{-1} H$_3$BO$_3$ (boric acid) prior to extraction chromatography. The distribution coefficient of Hf on TODGA is highly sensitive to the presence of trace amounts of HF (Fig. 3) and boron ions play a key role in fluorine complexation by restoring the affinity of the resin for Hf in nitric acid. High-purity boric acid crystals (Alfa Aesar®) dissolve readily when added directly to the sample solution. In contrast, the addition of boric acid is not necessary when LiBO$_2$ is used for sample digestion due to the presence of boron in the flux.

3.3. Vacuum cartridge extraction chromatography

The Eichrom vacuum box can accommodate up to 12 (or 24 in a larger model) samples at a time. An array of 10–20 mL syringe reservoirs, Eichrom resin cartridges and two disposable pipette tips were stacked on the box and vacuum was established (typical range 0.1–15 in Hg) using a single-stage Venturi pump (Mcmaster Carr, Cat# 41605K13) and air or nitrogen gas. The flow rates of acids through the column were controlled by adjusting the vacuum with a regulator. The typical flow rate for pre-conditioning and rinsing to remove matrix elements is 2–3 mL min^{-1}. The flow rates for the load solution and elution of elements should not exceed 2 mL min^{-1} to ensure maximum element recovery.

The vacuum cartridge extraction chromatography has several advantages over slurry-packed gravity columns: (a) flow rates as high as 3 mL min^{-1} can be used without compromising matrix removal and elemental separation (such high flow rates are not possible with conventional gravity columns), (b) the flow rate can be easily controlled by adjusting the vacuum during resin condition-

ing, matrix removal and sample elution, (c) many cartridges with different resins can be stacked in tandem to accommodate separation of multiple elements in a single load of sample solution. High distribution coefficients allow single-stage separation schemes that eliminate additional purification steps, and finally (e) sample contamination is minimized by isolating the elution vials inside the sealed vacuum box.

3.3.1. Separation of Ca, U, Th, Hf, Lu and Yb

In order to establish the chromatographic behavior of Ca, U, Th, Hf, Lu, Yb and matrix elements, elution experiments on TODGA and Ln-Spec resin were carried out. A multi-element standard solution was prepared from single and multi-element standard solutions with 34 elements at concentrations that were similar to natural samples. An aliquot of the standard solution was loaded onto the TODGA cartridge in 3 mol L^{-1} HNO$_3$ + 0.2 mol L^{-1} H$_3$BO$_3$. The recovery of all elements as a function of acid type, concentration and elution volume, are shown in Fig. 4. Lithium recovery, which is 100% at the end of the rinse step, is not shown due to the large amount of Li when LiBO$_2$ flux is used for sample digestion. The final extraction scheme for Ca, U, Th, Hf, Lu and Yb was optimized based on the partition coefficient of elements from Figs. 1–3 and multiple elution experiments. The acid concentration of the load solution on the TODGA was fixed at 3 mol L^{-1} HNO$_3$ in order to achieve concomitant sequestration of Ca, U, Th, Hf, Lu and Yb. Matrix elements, including alkali, alkaline earth and trace elements such as Ti and Fe, were removed from the resin during the load and subsequent rinse in 3 mol L^{-1} HNO$_3$. Calcium was quantitatively eluted in 11 mol L^{-1} HNO$_3$.

Although more than 90% of U and Th can be successfully eluted in 20 mL of 25 °C 3 mol L^{-1} HNO$_3$ + 0.2 mol L^{-1} HF (Fig. 4), significant tailing is observed with Hf and complete recovery requires up to 80 mL of the acid mixture. The possibility of increasing Hf yield by changing the temperature and HF concentration of the elution acid was explored. A conventional oven was used to heat 120 mL of 3 mol L^{-1} HNO$_3$ + 0.2 mol L^{-1} HF acid mixtures to 40, 50, 60 and 70 °C in PFA Teflon bottles. The TODGA cartridge and vacuum box were kept at room temperature (25 °C) throughout the experiment. For calibration purposes, Hf standard was loaded onto a 2-mL TODGA cartridge in 10 mL of 3 mol L^{-1} HNO$_3$ + 0.2 mol L^{-1} H$_3$BO$_3$. The load and elution flow rates were adjusted at ∼2 mL min^{-1} and Hf recovery was measured in 4 mL increments of the elution acids. Hafnium recovery as a function of acid temperature and elution volume is presented in Fig. 5. The total recovery is significantly improved (>90% in 20 mL) if the temperature of the elution acid is maintained at 60–70 °C. No traces of REEs were detected in the U, Th and Hf cut from the 70 °C acid. In contrast, increasing the concentration of HF to 0.5 mol L^{-1} did not significantly enhance the elution of Hf and trace amounts of REEs began to appear in the U–Th–Hf elution. The elution protocol for Hf (and U and Th) was therefore optimized by using 20 mL of 65 °C 3 mol L^{-1} HNO$_3$ + 0.3 mol L^{-1} HF.

Following U, Th and Hf elution, the light and middle REEs were eluted in 0.5 mol L^{-1} HCl (Fig. 4). Gadolinium, Tb and Dy partially co-elute with Lu and Yb and their oxides can interfere with Lu isotope dilution measurements. Although this issue can potentially be resolved by using an Apex-Q and Spiro TMD desolvating nebulizer, instead of a SIS inlet system, it is better to remove all interfering REEs from Lu and Yb prior to analysis using the Eichrom Ln-Spec resin [50]. In order to study the behavior of these elements on the Ln-Spec resin, a 2-mL Ln-Spec cartridge was preconditioned with 20 mL of 6 mol L^{-1} HCl, followed by 10 mL 0.05 mol L^{-1} HCl. A multi-standard solution of Gd, Tb, Dy, Lu and Yb was loaded to the cartridge in 10 mL of 0.05 mol L^{-1} HCl at a flow rate of ∼2 mL min^{-1}. Fig. 6 shows the recovery of Gd, Dy, Tb, Lu and Yb as a function of 100 mL of 3.5 mol L^{-1} HCl elution. Over 99% of Gd, Tb, Dy and ∼70%
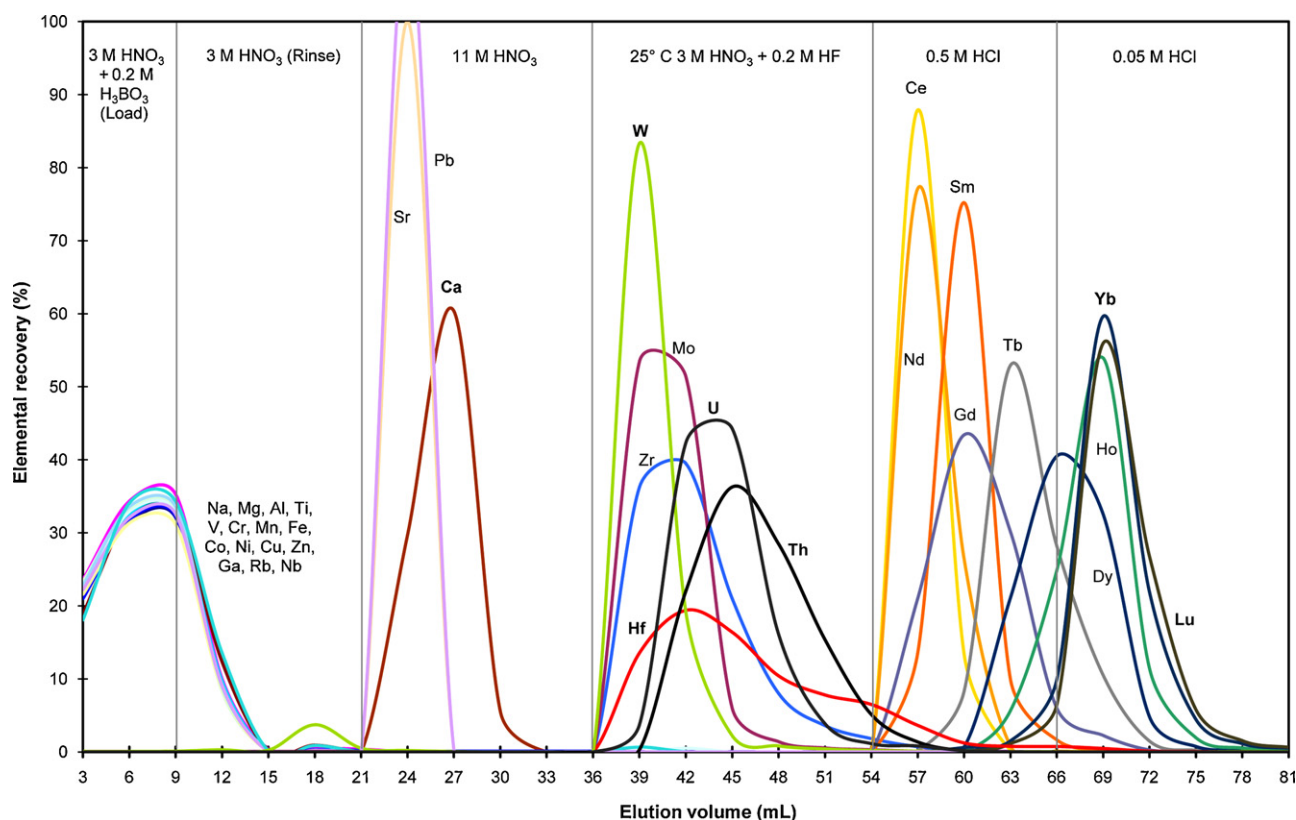
Fig. 4. Elution curves for 33 elements on a 2-mL cartridge (0.8 cm diameter, 2.5 cm length) of TODGA resin (50–100 μm particle size). The concentration of the load solution is fixed at 3 mol L^{-1} HNO$_3$ + 0.2 mol L^{-1} H$_3$BO$_3$ with HF bomb digestion, and 3 mol L^{-1} HNO$_3$ with flux fusion, to concomitantly retain Ca, U, Th, Hf and Lu on TODGA. Matrix elements are removed during the load, followed by rinse solutions in 3 mol L^{-1} HNO$_3$. Li recovery (not shown) was 100% at the end of 3 mol L^{-1} HNO$_3$ rinse step.

of Yb are eluted in the first 30 mL of 3.5 mol L^{-1}. After the initial separation, the remaining Yb and ∼70% of Lu can be eluted in 15–20 mL 6 mol L^{-1} HCl. A major advantage of this elution scheme is that Lu, Yb and overlapping residual REEs can be directly eluted from the TODGA cartridge (top) onto the Ln-Spec (bottom) in 0.05 mol L^{-1} HCl. This eliminates the need for time-consuming evaporation and dissolution to purify Lu and Yb, which may result in sample loss and contamination.

The combined analytical protocol for high-purity flux fusion and Ca, U, Th, Hf, Lu and Yb purification using the TODGA and Ln-Spec resin cartridges is summarized in Fig. 7. This procedure, which can be completed in less than a day, was utilized in the analysis of standard reference materials in the following sections.

3.3.2. Elemental recoveries in geostandards

In order to assess the efficiency of matrix separation and recovery of elements on the TODGA in natural samples, 10–100 mg of geostandard ANRT BX-N bauxite, USGS AGV-2 andesite, USGS BCR-2 basalt and CRPG AC-E granite were digested by flux fusion. The melt was directly transferred to 25 mL of 3 mol L^{-1} HNO$_3$ solution and loaded to the TODGA cartridge. Elemental separations were performed according to the scheme in Fig. 7 and the recoveries were calculated using standard bracketing technique on the Neptune. The elemental recoveries, presented in Table 3, were generally better than 92% for all elements.

3.4. High-precision concentration and isotope analyses

A detailed description of the ThermoFinnigan MC-ICP-MS can be found in Wieser et al. [4]. Faraday and SEM cup positions for Ca, Hf, U, Th and Lu isotopes and isobaric interferences that were monitored are shown in Table 4. A combination of static and dynamic

modes and Faraday and secondary electron multiplier (SEM) collectors were employed in medium and low mass resolutions. ESI quartz SIS spray chamber and ESI Apex-Q + Spiro TDM inlet systems were used for sample introduction. Apex heater and cooler temperatures were set at 140 and 2 °C, respectively. Nitrogen and Ar sweep gases for the Apex and Spiro were adjusted manually to achieve optimum intensity and stability of the ion signals at the beginning of each analysis session. All sample and standard solutions were introduced to the instrument through a PFA Teflon self-aspirating nebulizer with a nominal flow rate of 100 μL min^{-1}. Baseline and amplifier gain calibrations were performed daily prior to the analyses. The intensities of ions in the dilution acid solution measured at the beginning of each sequence were subtracted from all subsequent sample and standard measurements.

Isotopic abundances can vary following the laws of mass dependent fractionation. In particular, MC-ICP-MS is known to create a large instrumental mass bias towards heavier isotopes [1,51]. In the current study, we account for the mass fractionation of Hf, U, Th, Lu and Yb isotopes using the exponential law [38]:

$$R_t = R_m \left(\frac{M_2}{M_1} \right)^{\beta} \tag{3}$$

R_t and R_m represent the true (accepted) and measured isotopic ratios of masses M_2 and M_1, respectively. β is the mass bias coefficient, a free parameter that is determined experimentally.

3.4.1. Ca analysis

The Ca elution fraction (Fig. 7, step 10) was gravimetrically diluted to a solution of 0.5 mol L^{-1} HNO$_3$ and the concentrations were determined using the standard bracketing procedure. Calcium isotopes were measured in medium resolution mode using the
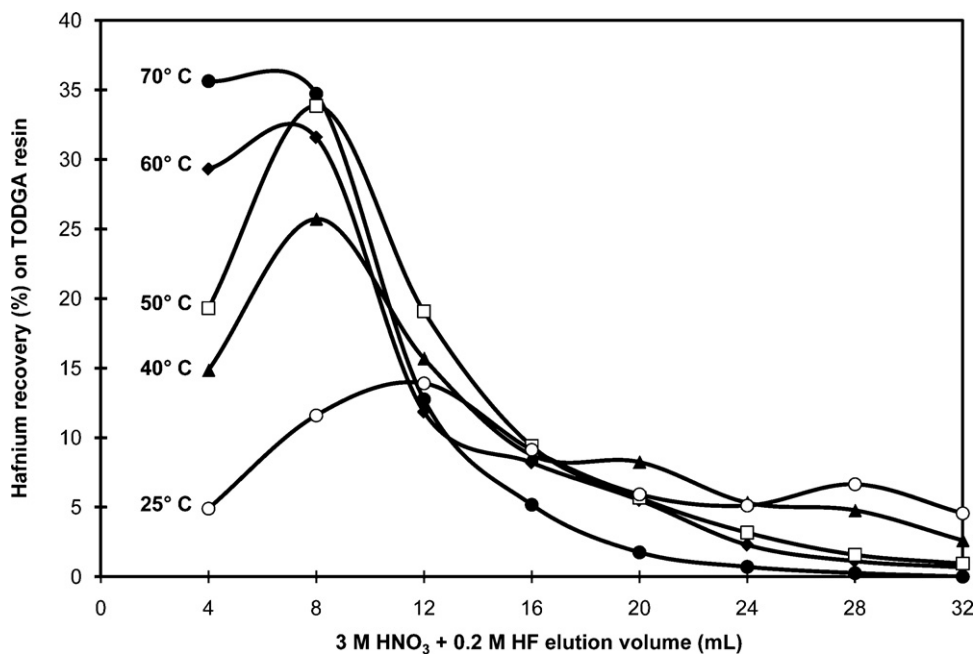
Fig. 5. Temperature effect on the recovery of Hf from TODGA in 3 mol L^{-1} HNO$_3$ + 0.2 mol L^{-1} HF. Hafnium standard was loaded in 10 mL of 3 mol L^{-1} HNO$_3$ + 0.2 mol L^{-1} H$_3$BO$_3$ and the flow rate was ~2 mL min^{-1}. The elution acids were heated in 125 mL PFA Teflon bottles inside a conventional oven and were loaded onto the resin in increments of 4 mL. The vacuum box and TODGA cartridge were kept at room temperature. Higher acid temperatures dramatically enhanced the recovery of Hf, while no traces of lanthanides were detected in the Hf cut as a result of temperature increase.
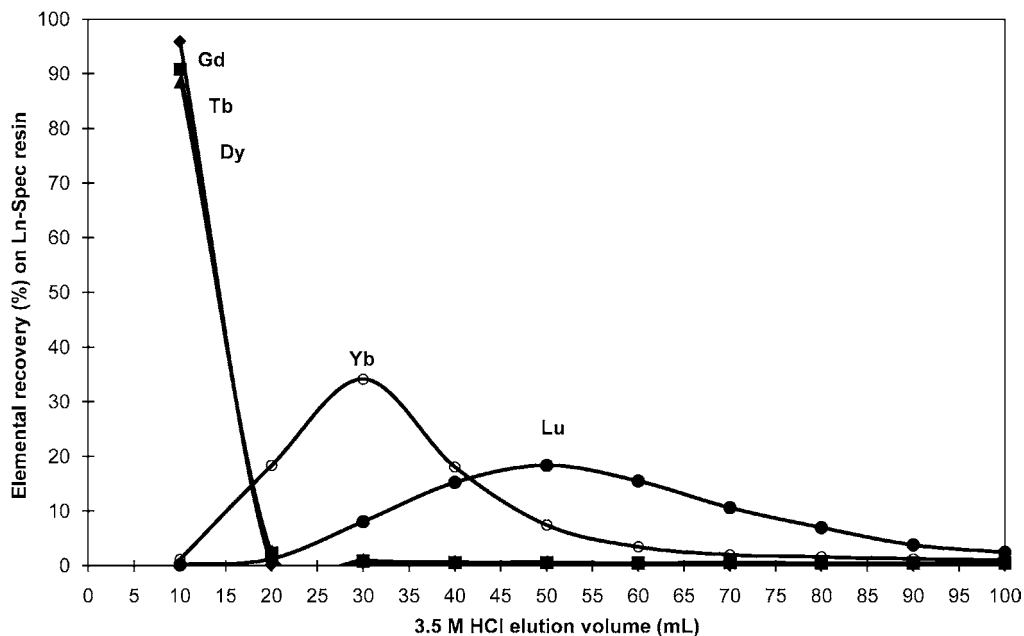

Fig. 6. Separation of Gd, Tb, Dy, Lu and Yb on a 2-mL Ln-Spec cartridge in 100 mL of 3.5 mol L^{-1} HCl elution. The cartridge was preconditioned with 20 mL of 6 mol L^{-1} HCl, followed by 10 mL 0.05 mol L^{-1} HCl to convert to load acid condition. The multi-standard solution was loaded in 10 mL of 0.05 mol L^{-1} HCl. Approximately 70% of Yb can be separated from Lu with 30 mL of 3.5 mol L^{-1} HCl.

Table 3
Elemental recoveries for geostandards digested with flux fusion and separated with TODGA extraction chromatography.

Element	Recovery (%)					
	AC-E	AGV-2	BCR-2	BX-N	Standard solution	Average geostandard
Lu	94	81	100	97	91	93
Hf	100	100	100	95	82	99
Th	93	99	100	101	100	98
U	93	94	86	96	100	92
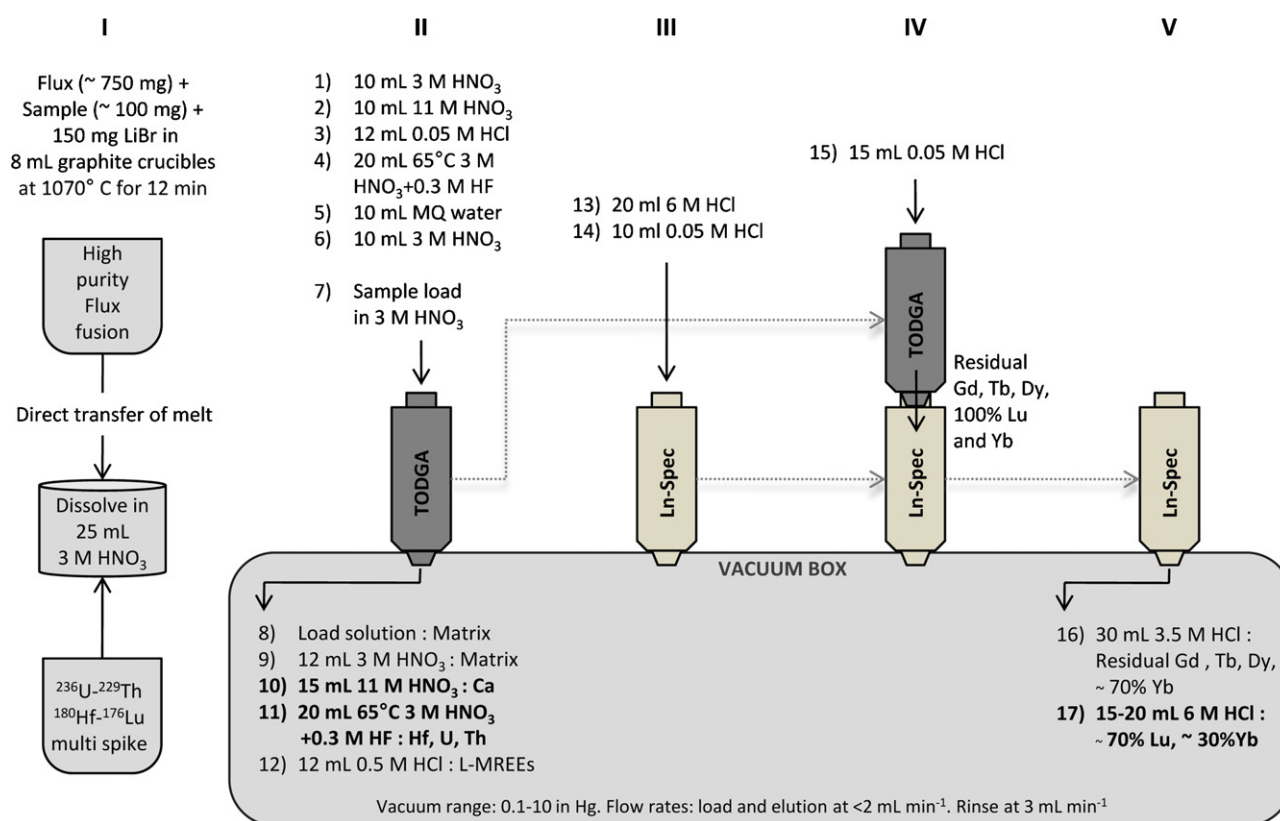
Fig. 7. High-purity flux fusion and extraction chromatography protocol for separation and purification of Ca, Hf, U, Th and Lu with Eichrom TODGA and Ln-Spec cartridges, used in tandem, on a vacuum box. Resin impurities are removed during the pre-conditioning steps. The elution of the elements of interest in this study is shown in bold. The entire procedure from flux fusion to preparation for ICP-MS analysis can be completed in 1 day.

30 μm entrance slit to avoid molecular interferences (*e.g.*, hydrides of Ar, N_2, N_2O, N_3 and CO_2) and a modified protocol from Wieser et al. [41] for collector configuration and instrument optimization. Titanium-47 was monitored for potential isobaric interference of ^{48}Ti on ^{48}Ca (Table 4). Although the intensity of ^{44}Ca was preferred to calculate concentrations, ^{42}Ca, ^{43}Ca or ^{48}Ca intensities produced identical results within analytical error, indicating that all other isotopes were free from interferences as well. Results from internal normalization by doping Ca sample and standard solutions with a Sc standard were similar to standard bracketing within error. The analysis method consisted of 1 block of 8 cycles of 4.2 s integration time, and samples were measured four times within each session.

The Ca concentration results for replicate analyses of USNM3529 using purified flux fusion in high-purity graphite crucibles and HF bomb digestion are presented in Table 5. Total procedural blank ($n=2$) for Ca using flux fusion was 1.6 μg and represented less than 0.1% of the Ca signal in the samples. The average Ca concentration based on all replicate analyses is 18.50 ± 0.14 mg g^{-1} (95% ci), which is in very good agreement with the recommended value of 18.44 ± 0.25 mg g^{-1} (95% ci) [52]. Although Ca concentra-

tions in replicate analyses of the samples digested with flux fusion are slightly lower than those of HF bomb dissolution, the results from each method of digestion are comparable within the analytical error.

3.4.2. U and Th analyses

Despite the importance of improving the current estimate of the cosmic Th/U ratio [53], replicate U and Th concentration data for Smithsonian Institute Allende reference material are surprisingly scarce [54–56]. The concentrations of U and Th in replicate digestions of USNM3529 were measured by isotope dilution on a 10% aliquot from the U–Th–Hf elution fraction (Fig. 7, step 11). Sample and standard solutions were introduced in 0.4 mol L^{-1} HNO$_3$ + 0.04 mol L^{-1} HF through the ESI Apex-Q + Spiro TDM inlet system to achieve high sensitivity. Isotope measurements were made in dynamic mode with ^{236}U and ^{229}Th ion beams on the SEM and ^{235}U, ^{238}U and ^{232}Th on Faraday collectors (Table 4). Faraday and SEM yield calibration was performed manually, using a NIST SRM4321c U standard solution (courtesy of Franco Marcantonio) with a pre-determined ^{238}U/^{235}U ratio of 137.90. Instrumental

Table 4

Faraday and SEM collector configurations for Ca, Hf, U, Th and Lu isotope analyses using the Neptune MC-ICP-MS. Calcium isotopes were measured in medium resolution. Isotopes ^{236}U and ^{229}Th were measured with the SEM in dynamic mode.

Element	Faraday and SEM cup positions									
	L4	L3	L2	LI	SEM	Axial	HI	H2	H3	H4
Ca	^{42}Ca		^{43}Ca	^{44}Ca			^{45}Sc		^{47}Ti	^{48}Ca
Hf	^{172}Yb	^{174}Hf	^{175}Lu	^{176}Hf		^{177}Hf	^{178}Hf	^{179}Hf	^{180}Hf	^{184}W
U				^{235}U	^{236}U		^{238}U			
Th					^{229}Th			^{232}Th		
Lu		^{171}Yb	^{172}Yb	^{173}Yb		^{174}Yb	^{175}Lu	^{176}Lu	^{177}Hf	

mass bias for U and Th isotopes was established according to equation (3) and a standard-sample-standard bracketing sequence using SRM4321c as the U standard. The instrumental mass bias based on the U standard solution ($n = 75$) at $\sim$10 ng g^{-1} was

determined to be 0.73% amu^{-1}. The abundance sensitivity of the Neptune without a Retardation Potential Quadrapole lens was $\sim$5 ppm amu^{-1} between ^{238}U and ^{237}U masses. Considering that the ^{238}U/^{236}U and ^{232}Th/^{229}Th ratios in spiked samples were typi-

Table 5
Elemental concentrations and isotope ratios of Ca, Hf, U, Th and Lu in Smithsonian Institute Allende reference powder (USNM3529 split 8, position 5) and USGS BCR-2, BHVO-1, AGV-1 and AGV-2 geostandards. Analytical precisions on the mean of concentrations and elemental ratios are reported as 95% confidence interval (95% ci), based on replicate analyses. Uncertainties on ^{176}Hf/^{177}Hf ratios (95% ci) were calculated from the dispersion of JMC-475 in each analysis session. Average ^{176}Hf/^{177}Hf for JMC-475 ($n = 150$, 10 ppb) was 0.282159 $\pm$ 3 (2SD$\sqrt{n}$). All ^{176}Hf/^{177}Hf ratios are normalized to the recommended JMC-475 value of 0.282160. Uranium, Th, Lu and Hf concentrations are from IDMS analyses, excluding results from Shinotsuka et al. [54], where standard calibration curve was used (1σ error). Calcium concentrations are measured by standard bracketing method.

Sample	Digestion method	U (ng g⁻¹)	Th (ng g⁻¹)	Ca (mg g)	Lu (μg g⁻¹)	Hf (μg g⁻¹)	¹⁷⁶Hf/¹⁷⁷Hf	¹⁷⁶Lu/¹⁷⁷Hf	Th/U	Reference
Current study										
USNM3529										
Allende (1)	GCPF[a]	15.34	58.19	18.36	0.0460	0.192	0.282835 ± 23	0.0339	3.79	This study
Allende (2)	GCPF	16.00	58.04	18.55	0.0459	0.192	0.282795 ± 15	0.0339	3.63	This study
Allende (3)	GCPF	15.71	58.90	18.38	0.0452	0.189	0.282839 ± 19	0.0338	3.75	This study
Allende (4)	GCPF	15.38	59.75	18.26	0.0485	0.206	0.282814 ± 19	0.0335	3.88	This study
Allende (5)	GCCF[b]	High blank	High blank		0.0468	0.194	0.282806 ± 26	0.0343		This study
Allende (6)	PtCCF[c]	High blank	High blank		0.0459	0.191	0.282808 ± 15	0.0340		This study
Allende (7)	PtCCF	High blank	High blank		0.0456	0.189	0.282820 ± 15	0.0342		This study
Allende (8)	HF Bomb	15.58	59.80	18.41	0.0460	0.193	0.282824 ± 25	0.0338	3.84	This study
Allende (9)	HF Bomb	15.23	58.37	18.79	0.0464	0.193	0.282795 ± 30	0.0342	3.83	This study
Allende (10)	HF Bomb	15.57	57.42	18.77	0.0461	0.192	0.282801 ± 30	0.0340	3.69	This study
Allende (11)	HF Bomb				0.0460	0.192	0.282815 ± 15	0.0340		This study
Mean		15.54 ± 0.23	58.64 ± 0.80	18.50 ± 0.14	0.0462 ± 8	0.193 ± 4	0.282814 ± 10	0.0340 ± 2	3.77 ± 0.08	This study
Geostandards										
BCR-2 (1)	HF Bomb				0.502	4.940	0.282855 ± 13	0.01440		This study
BCR-2 (2)	HF Bomb				0.503	4.963	0.282857 ± 8	0.01437		This study
BCR-2 (3)[d]	HF Bomb						0.282865 ± 11			This study
BCR-2 (4)[d]	GCCF						0.282867 ± 9			This study
Mean					0.502 ± 25	4.952 ± 50	0.282861 ± 8	0.01438 ± 7		This study
BHVO-1 (1)	HF Bomb				0.278	4.469	0.283097 ± 13	0.00881		This study
BHVO-1 (2)	HF Bomb				0.277	4.472	0.283097 ± 15	0.00878		This study
BHVO-1 (3)[d]	HF Bomb						0.283100 ± 11			This study
BHVO-1 (4)[d]	GCCF						0.283098 ± 9			This study
Mean					0.277 ± 15	4.471 ± 7	0.283098 ± 2	0.00880 ± 6		This study
AGV-I[d]	GCCF						0.282974 ± 9			This study
AGV-2[d]	GCCF						0.282981 ± 9			This study
Literature values										
USNM Allende										
Allende (1)	HF Bomb				0.0456	0.191	0.282816 ± 18	0.0339		[49] [e]
Allende (2)	HF Bomb				0.0457	0.190	0.282824 ± 5	0.0340		[49] [e]
Allende (1)	HF Bomb				0.0496	0.206	0.282828 ± 17	0.0341		[60] [f]
Allende (2)	HF Bomb				0.0481	0.198	0.282834 ± 16	0.0344		[60] [f]
Allende	Hot Plate				0.0461	0.192	0.282825 ± 11	0.0341		[58] [g]
Mean					0.0470 ± 20	0.195 ± 77	0.282825 ± 8	0.0341 ± 2		
Allende (1)	Hot Plate	15.6	57.9						3.71	[54] [h]
Allende (2)	Hot Plate	14.9	62.1						4.17	[54] [h]
Allende (3)	Hot Plate	15.6	65.3						4.19	[54] [h]
Allende	HF Bomb	15.3	62.2						4.07	[55] [i]
Allende	Hot Plate								3.43	[56] [j]
Mean		15.35 ± 1.85	61.88 ± 4.22						3.91 ± 0.38	
Allende ($n = 16$)				18.44 ± 0.	25					[52] [k]
Geostandards										
BCR-2	HF Bomb						0.282862	0.01436		[57]
BCR-2 ($n = 2$)	GCCF				0.499	4.967	0.282875 ± 7	0.01435		[39]
BCR-2 ($n = 4$)	HF Bomb				0.504	4.985	0.282869 ± 4	0.01435		[32]
BCR-2[d] ($n = 10$)	HF Bomb						0.282870 ± 8			[55]
BCR-2[d]	HF Bomb						0.282859 ± 9			[48]
Mean					0.501 ± 10	4.976 ± 39	0.282867 ± 7	0.01435 ± 1		
BHVO-1	HF Bomb						0.283096	0.00878		[57]
BHVO-1 ($n = 8$)	GCCF				0.279	4.512	0.283105 ± 4	0.00877		[39]
BHVO-1 ($n = 7$)	GCCF				0.261	4.230	0.283108 ± 8	0.00877		[32]
BHVO-1 ($n = 7$)	HF Bomb						0.283106 ± 12			[55]
BHVO-1 (1)	HF Bomb				0.28	4.48	0.283080 ± 5	0.00890		[59]
BHVO-1 (2)	HF Bomb				0.28	4.45	0.283076 ± 5	0.0090		[59]
BHVO-1 (3)[d]	HF Bomb						0.283090 ± 4			[59]
BHVO-1[d]	HF Bomb						0.283109 ± 4			[62]
Mean					0.275 ± 13	4.418 ± 177	0.283096 ± 11	0.00884 ± 12		

Table 5(*Continued*)

Sample	Digestion method	U (ng g^{-1})	Th (ng g^{-1})	Ca (mg g)	Lu (μg g^{-1})	Hf (μg g^{-1})	^{176}Hf/^{177}Hf	^{176}Lu/^{177}Hf	Th/U	Reference
AGV-1[d] (*n* = 5)	HF Bomb						0.282980 ± 5			[61]
AGV-2[d] (*n* = 6)	HF Bomb						0.282980 ± 15			[61]

[a] GCPF: Flux fusion in graphite crucible with purified LiBO$_2$ flux.
[b] GCCF: Flux fusion in graphite crucible with commercial grade LiBO$_2$ flux.
[c] PtCF: Flux fusion in Pt crucible with commercial LiBO$_2$ flux.
[d] Ratios are from unspiked material.
[e] USNM3529.
[f] USNM3529 split 17, position 16.
[g] USNM 3529 split. 7, position 3.
[h] USNM split 11, position 11.
[i] USNM split 20, position 29.
[j] USNM3529 split 9, position 2.
[k] USNM analyses by neutron activation, gravimetric and XRF methods.

cally in the range of 1–3 and 100–150, respectively, ^{238}U and ^{232}Th tail contributions to lower-abundance isotopes were negligible. The measurement method consisted of 1 block of 5 cycles of 4.2 s integration time, and each sample was measured twice within the run session. Mass bias and interference corrections were performed offline.

As shown in Table 2, blank contributions from commercial flux and Pt crucible digestions were considerably high and comprised of up to 50% of the sample signal. The analyses that required a large blank correction (higher than external reproducibility) were discarded. Total procedural blanks from purified flux fusion digestions for U and Th were 10 and 13 pg (*n* = 2), respectively. Results for U and Th concentrations and Th/U weight ratios are presented in Table 5. The mean of U and Th concentrations for seven replicate analyses determined by isotope dilution are 15.54 ± 0.23 and 58.64 ± 0.80 ng g^{-1}, respectively, with a mean Th/U ratio of 3.77 ± 0.08 (95% ci). The relative dispersion of Th/U ratios in Allende reference material in this study is ~4.8% (2σ), which is a significant improvement from 16.8% (2σ) reported by other investigators (Table 5). Such external reproducibility is sufficient to study Th/U variations in meteoritic materials as this ratio can vary by as much as 300% in bulk carbonaceous chondrites [36]. The mean Th/U ratio of 3.77 for homogenized Allende standard powder is close to the proposed average solar system value of *ca.* 3.7 [56] and, to our knowledge, represent the best available value for the USNM3529 Allende reference material.

3.4.3. Hf and Lu analyses

The U–Th–Hf eluate was split into two fractions. As mentioned above, approximately 10% was used for determination of U–Th concentrations by isotope dilution and Hf analyses were performed on the remaining solution (90%). After converting to 0.4 mol^{-1} HNO$_3$ + 0.04 mol^{-1} HF, the sample solution containing Hf was introduced to the mass spectrometer through the ESI Apex-Q + Spiro inlet system with a self-aspirating, 100 μL min^{-1} Teflon nebulizer.

Hafnium concentration and isotopic composition were measured using the cup configuration shown in Table 4. All isotopes were measured with the 10^{11} Ω amplifiers, except for the low-abundance isotope ^{174}Hf, which was measured with the 10^{12} Ω amplifier. The signal intensity for ^{176}Hf was maintained above 0.1×10^{-11} A because ^{176}Hf/^{177}Hf reproducibility exceeded 1ε (parts per ten thousand) at intensities below this level. Data was collected in 1 block of 15 cycles of 8.4 s integration time in static mode and every sample was measured up to three times within each analysis session. Instrumental mass bias was corrected by internal normalization to ^{179}Hf/^{177}Hf of 0.7325 using the exponential law (Eq. (3)). Instrumental drift was monitored by standard-sample-standard bracketing technique with a solution of 10 ng g^{-1} JMC-475 Hf isotope standard (courtesy of Jonathan Patchett, The University of Arizona). The unweighted mean ^{176}Hf/^{177}Hf

ratio for JMC-475 Hf standard analysis over the course of several sessions was 0.282159 ± 3 (2σ/$\sqrt{n}$, *n* = 150, last decimal place). This value is comparable to the JMC-475 ^{176}Hf/^{177}Hf ratios of 0.282144 ± 14 (*n* = 73) and 0.282154 ± 6 (*n* = 24) reported by Vervoort et al. [57] and Bouvier et al. [49], respectively. The masses of ^{175}Lu, ^{171}Yb and ^{184}W (and ^{181}Ta for select runs) were monitored within runs for the presence of isobaric interferences on ^{176}Hf and ^{180}Hf, and corrections were applied based on the natural abundances of interfering isotopes (^{176}Lu/^{175}Lu = 0.02658, ^{176}Yb/^{172}Yb = 0.5845, ^{180}W/^{184}W = 0.00391). The ^{175}Lu and ^{172}Yb ion intensities were at background level (<0.0001 × 10^{-11} A) on the Faraday cups, indicating a perfect separation of Hf from lanthanides on TODGA resin.

The ^{180}Hf/^{177}Hf ratio of the spike-sample mixture was used to calculate Hf concentrations by isotope dilution. The amount of spike added was adjusted so that the variation on ^{180}Hf/^{177}Hf was ~150ε for meteorite samples. The correction of ^{180}Ta on ^{180}Hf was negligible and ^{180}W ion beam represented less than 0.1% of the ^{180}Hf signal, which was nonetheless subtracted prior to Hf concentration calculations. An additional correction (up to 0.5ε) was also necessary on the ^{176}Hf/^{177}Hf ratio in USNM3529 samples from adding the enriched Hf spike. All measured ^{176}Hf/^{177}Hf ratios, corrected for mass bias and interferences, were normalized to the accepted JMC-475 value of 0.282160. The detailed calculations of isotope dilution, including offline corrections for isobaric interferences and instrumental mass bias, are provided as a Mathematica program (Electronic Supplementary Material).

Lutetium concentration was measured by isotope dilution on the eluate from the Ln-Spec cartridge that contained Lu and Yb (Fig. 7, step 17). There are only two naturally occurring isotopes of Lu (175 and 176), and although the mass bias (β) of Lu and Yb are not exactly the same, Yb isotopes are commonly used to monitor instrumental mass bias for determination of Lu concentration by isotope dilution [32,38,50,57–59]. It is therefore useful to keep some Yb in the Lu cut. Meanwhile, lowering the Yb/Lu ratio minimizes the ^{176}Yb (abundance 12.7%) correction on ^{176}Lu (abundance 2.59%). Doping experiments were performed by adding Yb to a Lu standard to determine the influence of Yb concentration on Lu isotopes. Increasing the Yb/Lu ratio to ~10 resulted in a 1.2% deviation of ^{176}Lu/^{175}Lu ratios from the true value after correcting for isobaric interference of ^{176}Yb on ^{176}Lu. Considering that elemental Yb/Lu ratios in meteorites and terrestrial rocks do not usually exceed 7, reducing the natural Yb/Lu ratio to <3 is sufficient for accurate measurements of Lu concentration by isotope dilution.

The solution containing Lu and Yb was introduced into the mass spectrometer in 0.4 mol L^{-1} HNO$_3$ through the Apex-Q + Spiro inlet system and a self-aspirating 100 μL min^{-1} Teflon nebulizer. All isotopes were measured with 10^{11} Ω amplifiers according to the cup configuration in Table 4. Data was collected in 1 block of 5 cycles

of 4.2 s integration time in static mode and each sample was measured twice within the analysis session. Different isotopes of Yb have been used here to calculate Lu mass bias [57]. The ^{173}Yb/^{171}Yb reference value of 1.132685 [59] was consistently used for internal normalization to calculate Lu mass bias.

The accuracy of Lu and Hf concentrations and isotope compositions was tested by measuring well-characterized geostandards. The results for replicate analyses of spiked and unspiked USNM3529 and USGS BCR-2, BHVO-1, AGV-1 and AGV-2 geostandards are presented in Table 5. Recommended values from literature are also presented for comparison. High-purity flux fusion and HF bomb results are similar within error, showing the effectiveness of the fusion method. The mean value for ^{176}Hf/^{177}Hf for all replicates of the Allende reference material is 0.282814 ± 10 (95% ci), which is identical, within error, to the average value of 0.282825 ± 8 (95% ci) based on five different analyses from the same Allende reference material by other investigators [49,58,60]. The mean of ^{176}Lu/^{177}Hf for 11 replicates of USNM3529 is 0.0339 ± 2 (95% ci), which is also similar, within error, to the mean value of 0.0341 ± 2 (95% ci) from the literature [49,58,60].

The mean ^{176}Hf/^{177}Hf and ^{176}Lu/^{177}Hf ratios for four BCR-2 replicates are 0.282861 ± 8 and 0.01438 ± 7 (95% ci), respectively and agree with the mean literature values of 0.282867 ± 7 and 0.01435 ± 1. The mean ^{176}Hf/^{177}Hf and ^{176}Lu/^{177}Hf ratios for four replicate analyses of BHVO-1 are 0.283098 ± 2 and 0.00880 ± 6 (95% ci), which are also consistent with the mean literature values of 0.283096 ± 11 and 0.00880 ± 12, respectively. The ^{176}Hf/^{177}Hf ratios for unspiked AGV-1 and AGV-2 are 0.282974 ± 9 and 0.282981 ± 9 (95% ci), respectively, and agree with literature values of 0.282980 ± 5 and 0.282980 ± 15.

In conclusion, the Hf isotopic compositions and Lu/Hf ratios for the standard reference materials, using HF bomb dissolution, purified borate flux fusion and the extraction chromatography protocol presented in Fig. 7, are all within recommended literature values (Table 5).

4. Summary

1. Replicate batch equilibration experiments were conducted to establish the distribution coefficients of 60 elements, including alkali, alkaline earth, transition and poor metals, lanthanides and actinides, on Eichrom TODGA resin in HCl, HNO$_3$ and HNO$_3$ + 0.2 mol L^{-1} HF. TODGA proved to be a highly versatile resin with an immense potential for matrix-analyte separation for high-precision elemental and isotope analysis of terrestrial and extraterrestrial material using ICP-MS.

2. The elution behavior of 34 and 5 representative elements were studied on the TODGA and Ln-Spec resins, respectively. A simple and robust protocol is proposed to separate Ca, U, Th, Hf, Lu, and Yb from the matrix with two TODGA and Ln-Spec cartridges utilized in tandem. High flow rates (>3 mL min^{-1}), unrivalled by conventional slurry-packed gravity columns, can be achieved with the use of a vacuum chamber.

3. High levels of blanks in alkali fluxes have been an impeding factor in using flux fusion as a method of choice to digest sample with refractory phases. A purification procedure is introduced to eliminate Hf, Th and U blanks in commercially available alkali fluxes (LiBO$_2$). The amounts of Hf, Th and U in the flux were reduced by over two orders of magnitude.

4. Multiple replicates of the Smithsonian Allende reference material and geostandards were analyzed for Ca, U, Th, Hf and Lu elemental and isotopic compositions using flux fusion, HF bomb dissolution and cartridge extraction chromatography. Results for flux fusion and HF bomb digestions were similar within error, proving the effectiveness of the method. The mean Th/U ratio

of seven replicate USNM3529 Allende analyses, measured by isotope dilution, is 3.77, which is close to the presumed solar system constant value of *ca.* 3.7. The Hf isotopic compositions and ^{176}Lu/^{177}Hf ratios of geostandards analyzed with our proposed protocol are in excellent agreement with recommended literature values.

Appendix A. Supplementary data

Supplementary data associated with this article can be found, in the online version, at doi:10.1016/j.talanta.2010.01.008.

References

[1] F. Albarède, P. Telouk, J. Blichert-Toft, M. Boyet, A. Agranier, B. Nelson, Geochim. Cosmochim. Acta 68 (2004) 2725.
[2] H.E. Gabler, J. Geochem. Explor. 75 (2002) 1.
[3] A.N. Halliday, D.C. Lee, J.N. Christensen, M. Rehkamper, W. Yi, X.Z. Luo, C.M. Hall, C.J. Ballentine, T. Pettke, C. Stirling, Geochim. Cosmochim. Acta 62 (1998) 919.
[4] M.E. Wieser, J.B. Schwieters, Int. J. Mass Spectrom. 242 (2005) 97.
[5] M. Rehkamper, M. Schonbachler, C.H. Stirling, Geostandard Newslett. 25 (2001) 23.
[6] F. Albarède, B. Beard, Rev. Minerol. Geochem. 56 (2004) 113.
[7] R.W. Carlson, E.H. Hauri, C.M.O.D. Alexander, in: J.G. Holland, S.D. Tanner (Eds.), Plasma Source Mass Spectrometry: The New Millennium, The Royal Society of Chemistry, Cambridge, 2001, p. 288.
[8] N. Dauphas, A. Pourmand, F.-Z. Teng, Chem. Geol. 267 (2009) 175.
[9] D.J. Douglas, S.D. Tanner, in: A. Montaser (Ed.), Inductively Coupled Plasmas Mass Spectrometry, Wiley-VCH, New York, 1998, p. 615.
[10] F.W.E. Strelow, Anal. Chem. 56 (1984) 1053.
[11] K.A. Kraus, G.E. Moore, J. Am. Chem. Soc. 71 (1949) 3263.
[12] J.P. Faris, Anal. Chem. 32 (1960) 520.
[13] W.G. Faix, R. Caletka, V. Krivan, Anal. Chem. 53 (1981) (1719).
[14] J.S. Fritz, T.A. Rettig, Anal. Chem. 34 (1962) 1562.
[15] F. Nelson, T. Murase, K.A. Kraus, J. Chromatogr. 13 (1964) 503.
[16] F.W.E. Strelow, R. Rethemey, C.J.C. Bothma, Anal. Chem. 37 (1965) 106.
[17] E.P. Horwitz, M.L. Dietz, D.M. Nelson, J.J. Larosa, W.D. Fairman, Anal. Chim. Acta 238 (1990) 263.
[18] E.P. Horwitz, M.L. Dietz, R. Chiarizia, H. Diamond, A.M. Essling, D. Graczyk, Anal. Chim. Acta 266 (1992) 25.
[19] B. Le Fevre, C. Pin, Anal. Chim. Acta 543 (2005) 209.
[20] Y. Nebel-Jacobsen, E.E. Scherer, C. Münker, K. Mezger, Chem. Geol. 220 (2005) 105.
[21] C. Pin, J.F.S. Zaldueguí, Anal. Chim. Acta 339 (1997) 79.
[22] A. Pourmand, F. Marcantonio, T.S. Bianchi, E.A. Canuel, E.J. Waterson, Paleoceanography 22 (2007).
[23] S. Weyer, A.D. Anbar, A. Gerdes, G.W. Gordon, T.J. Algeo, E.A. Boyle, Geochim. Cosmochim. Acta 72 (2008) 345.
[24] S.L. Maxwell, J. Radioanal. Nucl. Chem. 275 (2008) 497.
[25] C. Munker, S. Weyer, E. Scherer, K. Mezger, Geochem. Geophys. Geosyst. 2 (2001).
[26] K. Van Hecke, G. Modolo, J. Radioanal. Nucl. Chem. 261 (2004) 269.
[27] H. Hoshi, Y.Z. Wei, M. Kumagai, T. Asakura, Y. Morita, J. Alloys Compd. 374 (2004) 451.
[28] S.A. Ansari, P.N. Pathak, M. Husain, A.K. Prasad, V.S. Parmar, V.K. Manchanda, Talanta 68 (2006) 1273.
[29] A. Zhang, E. Kuraoka, M. Kumagai, Sep. Purif. Technol. 54 (2007) 363.
[30] J.N. Connelly, Geochem. Geophys. Geosyst. 7 (2006).
[31] S.L. Maxwell, J. Radioanal. Nucl. Chem. 275 (2008) 395.
[32] J.N. Connelly, D.G. Ulfbeck, K. Thrane, M. Bizzarro, T. Housh, Chem. Geol. 233 (2006) 126.
[33] E.P. Horwitz, D.R. McAlister, A.H. Bond, R.E. Barrans, Solvent Extr. Ion Exc. 23 (2005) 319.
[34] Y. Amelin, D.C. Lee, A.N. Halliday, R.T. Pidgeon, Nature 399 (1999) 252.
[35] T. van de Flierdt, S.L. Goldstein, S.R. Hemming, M. Roy, M. Frank, A.N. Halliday, Earth Planet. Sci. Lett. 259 (2007) 432.
[36] A. Rocholl, K.P. Jochum, Earth Planet. Sci. Lett. 117 (1993) 265.
[37] M. Frank, Rev. Geophys. 40 (2002).

[38] J. Blichert-Toft, C. Chauvel, F. Albarède, Contrib. Mineral. Petr. 127 (1997) 248.
[39] M. Bizzarro, J.A. Baker, D. Ulfbeck, Geostandard Newslett. 27 (2003) 133.
[40] C. Pin, J.S. Zalduegui, Anal. Chim. Acta 339 (1997) 79.
[41] M.E. Wieser, D. Buhl, C. Bouman, J. Schwieters, J. Anal. Atom. Spectrom. 19 (2004) 844.
[42] I.C. Kleinhanns, K. Kreissig, B.S. Kamber, T. Meisel, T.F. Nagler, J.D. Kramers, Anal. Chem. 74 (2002) 67.
[43] P. Rodriguez-Gonzalez, J.M. Marchante-Gayon, J.I.G. Alonso, A. Sanz-Medel, Spectrochim. Acta B 60 (2005) 151.
[44] K.G. Heumann, in: F. Adams, R. Gijbels, R. van Grieken (Eds.), Inorganic Mass Spectrometry, Wiley, New York, 1988, pp. 301–376.
[45] D. Ulfbeck, J. Baker, T. Waight, E. Krogstad, Talanta 59 (2003) 365.
[46] N.J. Mahlen, B.L. Beard, C.M. Johnson, T.J. Lapen, Geochem. Geophys. Geosyst. 9 (2008).
[47] J.T. Wasson, G.W. Kallemeyn, Philos. T. Roy. Soc. Lond. A 325 (1988) 535.
[48] T.J. Lapen, N.J. Mahlen, C.M. Johnson, B.L. Beard, Geochem. Geophys. Geosyst. 5 (2004).
[49] A. Bouvier, J.D. Vervoort, P.J. Patchett, Earth Planet. Sci. Lett. 273 (2008) 48.
[50] J. Blichert-Toft, Geostandard Newslett. 25 (2001) 41.
[51] C.N. Marechal, P. Telouk, F. Albarède, Chem. Geol. 156 (1999) 251.
[52] E. Jarosewich, R.S. Clarke Jr., J.N. Barrows, Sm. C. Earth Sci. 27 (1987).
[53] N. Dauphas, Nature 435 (2005) 1203.
[54] K. Shinotsuka, H. Hidaka, M. Ebihara, Meteoritics 30 (1995) 694.
[55] M. Tatsumot, R.J. Knight, C.J. Allegre, Science 180 (1973) 1279.
[56] J.S. Goreva, D.S. Burnett, Meteor. Planet. Sci. 36 (2001) 63.
[57] J.D. Vervoort, P.J. Patchett, U. Soderlund, M. Baker, Geochem. Geophys. Geosyst. 5 (2004).
[58] J. Blichert-Toft, F. Albarède, Earth Planet. Sci. Lett. 148 (1997) 243.
[59] N.C. Chu, R.N. Taylor, V. Chavagnac, R.W. Nesbitt, R.M. Boella, J.A. Milton, C.R. German, G. Bayon, K. Burton, J. Anal. Atom. Spectrom. 17 (2002) 1567.
[60] P.J. Patchett, J.D. Vervoort, U. Soderlund, V.J.M. Salters, Earth Planet. Sci. Lett. 222 (2004) 29.
[61] D. Weis, B. Kieffer, D. Hanano, I.N. Silva, J. Barling, W. Pretorius, C. Maerschalk, N. Mattielli, Geochem. Geophys. Geosyst. 8 (2007).
[62] J. Blichert-Toft, J.D. Gleason, P. Telouk, F. Albarède, Earth Planet. Sci. Lett. 173 (1999) 25.